Analysis and removal of multiply scattered tube waves

Gérard C. Herman [*] Paul A. Milligan [†] Qicheng Dong [‡]
James W. Rector III [§]

February 12, 1998

Abstract

Due to irregularities in or near the borehole, VSP or cross-well data can be contaminated with scattered tube waves. This type of organized noise can not always be removed with filtering methods currently in use. We propose a method, based on a one-dimensional impedance scattering model, for suppressing scattered tube waves. This method also accounts for multiply scattered tube waves. We apply the method to an actual VSP dataset and conclude that the continuity of reflected events is improved significantly in a washout zone.

Running title: **Removal of scattered tube waves**

[*]Centre for Technical Geoscience, Delft University of Technology, Mekelweg 4, 2628 CD Delft, The Netherlands.

[†]Engineering Geoscience, Building 90, Room 2002, Lawrence Berkeley National Laboratory, University of California, Berkeley, CA 94270

[‡]Engineering Geoscience, Building 90, Room 2002, Lawrence Berkeley National Laboratory, University of California, Berkeley, CA 94270

[§]Department of Materials, Science & Mineral Engineering, University of California at Berkeley, 577 Evans Hall, Berkeley, CA 94270

1 Introduction

In many VSP or crosswell datasets, tube waves are the major source of coherent noise, leading to difficulty in separation of the reflected wavefield. For suppressing the direct tube wave, multichannel filters can be used. A method, based on polarization filtering, has been suggested by Campbell (1992). Alternative techniques for suppressing the direct tube wave have also been discussed, by, for instance, Houston (1992) and Ellefsen et al. (1993). Apart from the direct tube wave, however, scattered tube waves can also be present. Scattering of tube waves can be caused by irregularities in the diameter of the borehole like washout zones (Hardage, 1983) or by cross-sectional area changes in the borehole fluid column. In addition, lithology changes in the formation adjacent to the borehole can also cause scattering of tube waves (Peng, 1992). Experimental techniques for reducing the scattered tube waves have been suggested by Pham et al. (1993) and Milligan et al. (1997). In the case of large washout zones, however, these experimental methods are not always sufficient. In the present paper, a processing technique is suggested for reducing the effect of scattered tube waves. The theoretical basis of the method is a simple but effective one-dimensional scattering model of the borehole scattering process. It has been shown by Tezuka et al. (1997), that this type of method is accurate if the borehole diameter is small with respect to the seismic wavelengths involved, a condition that is satisfied for the frequencies used in VSP and many crosswell applications.

A numerical model study of tube-wave scattering

Before describing the method for suppressing the scattered tube waves, we first consider the tube-wave scattering problem in somewhat more detail with the aid of a modeling study. We consider a cross-hole geometry with the source at a distance of 21 m from the receiver well. In the receiver well, a washout zone is present having a vertical extent of 3 m, where the diameter of the borehole changes abruptly from 0.073 m to 0.1 m. The depth of

the washout zone is the same as the source depth. The peak frequency of the source is 500 Hz, the compressional wave speed, v_P, is 3,800 m/s, the density is 2 g/cc, the wave speed in the fluid of the receiver borehole is 1,500 m/s and the shear wave speed v_S satisfies the relation $v_S = 0.6\, v_P$. With the aid of the bi-domain finite-difference modeling method of Dong and Rector (1997), we have computed the pressure at various depths in the receiver well. The result is shown in figure 1. This figure shows the direct compressional wave in the region around the washout zone. Even though the diameter change is very small when compared to the wavelength, a significant amount of tube-wave scattering is caused by the two discontinuities at either side of the washout zone. The tube waves originated in this way, remain trapped in the washout zone for a while causing a major distortion of the direct arival. The washout zone acts as a resonator trapping tube-wave energy for some time before releasing it in the form of tube waves propagating away from it. A similar behavior can be observed for upcoming reflections propagated through low-velocity shallow subsurface anomalies (Combee, 1994). The linear tube-wave events outside the washout zone can be reduced with the aid of multichannel filters, but the horizontal event in the washout zone itself can not be removed in this way without affecting the direct wave. Apart from the direct wave, upcoming reflected waves can also be distorted in a similar way by scattered tube waves within the washout zone. The method to be discussed in the present paper mainly aims at removing this type of scattering effect. As is apparent from figure 1, the scattered tube waves are not weak with respect to the first arrival and can bounce a few times within the washout zone before they have been attenuated sufficiently. This implies that multiple scattering of the tube wave preferably has to be taken into account.

2 Description of the method

Scattering of tube waves by borehole washouts is a complicated process. Stephen et al. (1985) used a finite-difference approach to model this type of scattering problem numerically. Bouchon and Schmidt (1988) developed a boundary-integral equation method. More recently, Dong and Rector (1997) proposed a bi-domain finite-difference method for studying the effect of irregular boreholes for VSP and crosswell surveys.

For the frequencies used in most VSP and crosswell appications, the diameter of the borehole is such that only the fundamental mode of the Stoneley wave, often termed tube wave, is excited. This is a guided wave, which implies that most of the energy is trapped inside the borehole and has no spherical spreading. The pressure across the borehole can be assumed to be uniform (Tang and Cheng, 1993). This implies that, for this type of geometry, the propagation of tube waves can be approximated by a one-dimensional method (Tezuka et al., 1997). In this way, the above three-dimensional scattering problem can be approximated by a one-dimensional one, which forms the basis for the method of removing the scattered tube waves discussed in the present paper.

We decompose the pressure p, recorded in the borehole, in the following way:

$$p(z,\omega) = d(z,\omega) + r(z,\omega) \ , \tag{1}$$

where d is the direct compressional wave and r is the remaining field, consisting of, for instance, reflections and the direct tube wave from the top of the fluid column. The depth is denoted by z, whereas ω is the angular frequency. From now on, the dependence on ω is omitted for brevity. Outside the borehole, all field quantities are depending on the three spatial coordinates, but inside the borehole, lateral variations are neglected since the borehole is assumed have a sufficiently small diameter. Therefore, only the z dependence of all field quantities is taken into account. In the remainder, it is assumed that the direct arrival d is clearly separated in time from the reflections and remaining wavefield r. The

direct arrival d includes the local effect of scattering in washout zones and irregularities in or near the borehole. We now decompose this direct arrival in the following way:

$$d(z) = d^0(z) + d^1(z) \ , \tag{2}$$

where d^0 would be the direct wave without the effect of the irregularities and d^1 therefore accounts for the wavefield scattered by these irregularities. In many cases, one can make an "educated guess" for d^0 when the direct arrival is a dominant feature on the record. For instance, coherency filtering or other multichannel filtering methods can be used to obtain an estimate of the "undistorted" direct field d^0. The same type of separation is now also made for the total recorded pressure field p, i.e., we have:

$$p(z) = p^0(z) + p^1(z) \ , \tag{3}$$

where p^0 would be the total field without the effect of the irregularities and the scattered field p^1 accounts for these irregularities. **The objective of the method presented here is to obtain an estimate of the field** p^0 , i.e. the wavefield we would have had in the absence of irregularities. Since the total wavefield p is measured and therefore known, this amounts to estimating the scattered total wavefield p^1. In order to do this, we assume that the borehole scattering process can be expressed in the form

$$p^1(z) = \int_{\text{borehole axis}} g(z - z') \ \ \sigma(z') \ p(z') \ dz' \ , \tag{4}$$

where σ is the (depth- and frequency- dependent) scattering impedance of the borehole and g is the borehole Green's function. This type of impedance-scattering method has been succesfully applied for describing near-surface scattering of Rayleigh waves (Snieder, 1986a, 1986b, and Blonk and Herman, 1994). Its validity mainly depends on the fact that the heterogeneities are close to the borehole or that the diameter change due to the washout zone is small compared to the wavelength. The scattering-impedance model (4) in fact implies that all scattering processes are "lumped" at the borehole axis. The

formulation (4) is consistent with the one-dimensional formulation of Tezuka et al. (1997) who use a reflectivity-type formulation. In the Green's function g, or impulse response of the borehole, we only consider the part corresponding to the tube wave. This is valid, under the asumption that an impedance secondary scattering source, whether excited by an incident compressional, shear or tube wave, mainly emits scattered tube waves. This has been observed from numerical finite-difference simulations for realistic geometries (see, for instance, the example shown in figure 1) and is also evident in real data (section 3). Also for the case of near-surface scattering, it has been found that the guided-wave part of the scattered wavefield, the Rayleigh wave, is significantly larger than the other constituents (Blonk and Herman, 1994). More details on the Green's function g are given in the Appendix. It depends on the tube wave speed, c_T, which can be estimated fairly easily from the data. It is tempting to replace the total pressure under the integral by the undistorted pressure p^0, which is the Born approximation and is common practice in seismic imaging. However, for this particular case it is not necessary, since p is known whereas p^0 is the quantity to be determined. Furthermore, the scattered field p^1 is definitely not always small with respect to p which implies that the Born approximation is not valid in this case. Our choice implies that the scattering model described by Eqs. (3)-(4) includes multiply scattered tube waves.

If we now want to estimate p^1, we first have to estimate the scattering impedance σ since the total wavefield is known (measured), whereas a fair estimate of g is available after measuring the tube-wave speed c_T from the data. In order to estimate the scattering impedance, we therefore first concentrate on the direct arrival d. According to Eq.(2), the direct arrival can be decomposed into an undisturbed part d^0 and the scattered direct arrival d^1. In a similar way as expressed in Eq.(4), we can relate the scattered first arrival d^1 to the impedance, σ, and the Green's function, g, through the relation

$$d^1(z) = \int_{\text{borehole axis}} g(z - z') \;\; \sigma(z') \; d(z') \; dz' \; . \tag{5}$$

If we now assume that the first arrival can be separated from the data p, which implies that d is known, and that we have a way of estimating the undisturbed direct arrival d^0, for instance by attributing rapid variations in d to scattering, we can determine d^1 from Eq.(2). Then, we can estimate σ from Eq.(5) after which the scattered total field p^1 follows by evaluating Eq.(4). Step by step, the method is then as follows:

1. *Separation of the direct arrival d and determination of d^0*

   Separation of the direct arrival can be done by windowing the downgoing direct arrival in the seismic record. This window should be large enough to include the diffraction tails of the scattered direct arrival d^1 but, at the same time, small enough so it includes as little reflection energy or other mode-converted energy as possible. Determination of the undisturbed direct arrival d^0 is the first adaptive step of the method. In principle, d^0 can be determined with the aid of spatial filtering or smoothing techniques by assuming that all rapid variations in d can be attributed to tube-wave scattering. Of course, this is an approximation, but it captures the most dominant part of the scattering process.

2. *Determination of σ*

   After determining d and d^0, d^1 is known. After determining the tube wave speed from the seismogram, g is also known (see the Appendix). This is done in two steps. In the first step, we determine the quantity $\sigma\ d$ by evaluating the right-hand side of the equation:

$$\sigma(z')\ d(z') = \int_{\text{borehole axis}} h(z'-z)\ \ d^1(z)\ dz\ , \tag{6}$$

   where h is the inverse of the Green's function g, defined by the relation

$$\delta(z''-z') = \int_{\text{borehole axis}} h(z''-z)\ g(z-z')\ dz\ . \tag{7}$$

   The determination of h is best done after transforming g, given by Eq.(9), to the wavenumber domain with the aid of the spatial Discrete Fast-Fourier Transform,

after which h is found by a stabilized spectral division. Also the convolution in Eq.(6) is best done in the wavenumber domain. The latter step is in fact a spatial deconvolution for the tube-wave scattering operator. After obtaning $\sigma\ d$, we obtain σ by dividing the result in the frequency domain, by the known wavefield d. Like the spectral division by g, also the latter division has to be stabilized since it corresponds to a temporal deconvolution for the downgoing direct arrival.

3. *Determination and removal of the scattered total field* p^1

   When the borehole scattering impedance $\sigma(z,\omega)$ is known for each depth and frequency, the scattered total field p^1 can be computed with the aid of Eq.(4). Again, this spatial convolution is best done in the wavenumber domain. Finally, the undisturbed field p^0 can be estimated by subtracting p^1 in an adaptive way from p. This adaptive subtraction is the second adaptive element of this otherwise deterministic method.

3 Application to actual seismic data

Before applying the method to an actual data set, it has been validated first by applying it to simulated data where the undisturbed field was accurately known. For brevity, this validation is omitted and we concentrate ourselves on the application to an actual VSP dataset. The data has been recorded with a weight-drop source situated at a distance of 72 m from the receiver well. There were 146 hydrophone channels with a vertical spacing of about 0.5 m; the upper hydrophone was at a depth of 79 m. Apart from the fact that the subsurface around the well was very complex, the dataset had the additional difficulty of scattered tube waves. This data set was collected for imaging the shallow subsurface as part of an environmental site study and was configured with inter-element foam baffles to slow down and attenuate the tube waves scattered from the different elements (Milligan et al., 1997). This acquisition approach, however, could not be used to attenuate tube

waves scattered from washout zones.

In figure 2, a detail of the VSP is shown. In the area between 90 m and 96 m deep, there are scattered tube waves present, probably caused by a washout zone. After applying a frequency-wavenumber fan filter removing all slopes equal or larger than the slope of the tube wave, we obtain the result shown in figure 3. The linear tube-wave noise has been removed, but the apex is still present between 90 m and 96 m. Subsequently, after suppressing the downgoing direct arrival with the aid of a constrained eigenvector method (Mars and Rector, 1995), we obtain the result shown in figure 4. In the washout zone, remnants of the tube-wave apex are visible. The tube-wave remnants are confined principally to the washout zone and are smeared by the repeated spatial filtering. They are interfering with the upcoming waves and therefore destroying the continuity of reflections in the washout zone.

We have applied the method for tube-wave suppression, discussed in section 2, to this dataset. In the first step, the direct arrival (including the scattered part) is separated with the aid of a time window having a width of about 20 ms. Then, a narrow frequency-wavenumber filter is applied in order to retain only the linear part of the direct arrival. The result of this process is assumed to be the "undisturbed" direct arrival, d^0, that we would observe in the absence of the washout zone. This estimate of d^0 is shown in figure 5. After subtracting d^0 from the actual windowed first arrival, we obtain our estimate of the scattered first arrival, d^1. This scattered first arrival d^1, shown in figure 6, can be used for estimating the borehole scattering impedance $\sigma(z,\omega)$ in the second step of the method discussed in section 2. First, the product $\sigma\ d$ is determined by spatially convolving the scattered field d^1 with the inverse h of the tube-wave Green's function g, as given by Eq.(6). The value of $\sigma(z,\omega)$ is then obtained after a temporal deconvolution (or spectral division) for the actual downgoing wavefield d. The result for σ obtained in this way is shown in figure 7. When comparing this with the scattered field of figure 6, it indeed

seems more "focused". After the impedance distribution has been obtained from the direct arrival, we can apply it to estimate the total scattered field p^1 by evaluating the right-hand side of Eq.(4). By subtracting the estimate of p^1 obtained in this way from the total field p, we obtain the undisturbed field p^0, which would have been observed in the absence of the washout zone. This estimate p^0 is shown in figure 8 after application of a frequency-wavenumber fan filter for removing remnants of tube waves. All processing and display parameters are the same for figures 3 and 8, the only difference being that, in figure 8, the scattered tube waves have been suppressed with the impedance method discussed in this paper. The interference patterns due to remnants of the apex of the scattered tube waves have been reduced in figure 8. The fact that the patterns in the first arrival have been removed serves as "quality control", for this was the criterion for designing the impedance filters, but the fact that the interference patterns have also disappeared in events not used in deriving the filters, is an indication that the scattering model is correct. In figure 9, the result is shown after removing the downgoing events from the result of 8 in order to concentrate on the upcoming, reflected events. When we compare figure 9 with figure 4, we observe that the "wormy" interference patterns between 90 m and 96 m depth have been reduced whereas the continuity of upcoming events seems to have improved in figure 9. The remaining interference patterns of figure 9 are probably due to the interference of events of different dip caused by the rather complex geology around the well. The difference is also illustrated in figures 10 and 11 with more trace coverage above and below the washout zone. Note how some of the terminations of reflections have been weakened in figure 11 in the zone overlapping with the estimated undisturbed direct arrival, d^0, shown in figure 5. In this region, the assumption that the direct field, d, and the remaining field, r, are separated in time, is not satisfied.

4 Concluding remarks

In this paper, a method for reducing the effect of scattered tube waves has been presented. It is based on the following assumptions:

1. Tube-wave scattering and conversion of P- and S- waves into tube waves can be described by a one-dimensional impedance model. This implies that the scattering process has to take place close to the borehole.

2. The scattered tube waves are the dominant part of the scattered wavefield

3. The direct arrival is separated in time from the upcoming reflections. This means that terminations of reflections, that are interfering with the direct arrival, can in principle be attenuated by applying this method. We have observed this effect in our final results shown in figures 9 and 11. All deeper reflections, however, are treated correctly.

The impedance method discussed in this paper is not based on the Born approximation and therefore can take multiple tube-wave scattering into account. This seems necessary, since the Born approximation does not seem to be valid when scattered tube waves are strong enough compared to the total wavefield to be re-scattered multiple times (see figure 1). The method has been validated for synthetic data and tested on an actual VSP dataset. It appears to reduce the effect of mainly the apex of the scattered energy which can not be removed with the aid of conventional frequency-wavenumber filtering techniques or the like.

The method is in essence deterministic and based on wave theory but contains two important adaptive steps:

1. The determination of the direct arrival d by applying a time window to the data and, especially, the estimation of the undisturbed direct arrival d^0 from d by attributing rapid variations in d to the scattered field.

2. The adaptive subtraction of the estimate of the scattered total field, p^1, from the total field p in order to obtain the undisturbed total field p^0.

The improvement of the continuity of both downward and upward propagating events in washout zones can serve as a quality control check to make shure that the method does not act as a simple dip filter.

The method can be extended to the case of a multi-offset VSP. In principle, this can be done in two ways. The simplest way would be to remove the scattered tube waves for each shot record separately. A more consistent approach would be, however, to use several shot records simultaneously for deriving a single scattering impedance model. One could call this "borehole consistent". This requires a least-squares approach because of the overdetermined character of the problem and also an approach for equalizing the shot-to-shot variations by a shot-consistent procedure. Another extension would be the improvement of the estimation of the undisturbed direct wave, d^0. If terminations of reflections were removed prior to the estimation of d^0, these terminations would probably not be weakenend by the application of the impedance scattering method.

The near-receiver scattering problem considered here shows a remarkable resemblance to the near-subsurface "statics" problem (see, for instance, Combee, 1994). Since shallow scattering problems can also be cast into a scattering-impedance formulation, one could apply a similar formalism to resolve near-receiver scattering effects also known as "short-wavelength" statics (mutatis mutandis), and again a similar method for resolving the near-source effects. Instead of the tube-wave part of the Green's function, one would probably need the Rayleigh-wave part.

5 Acknowledgments

This research has been carried out while Gérard Herman was a Phoebe Apperson Hearst visiting professor in the Department of Materials Science and Mineral Engineering with

the financial support of the University of California at Berkeley and the Dutch Technology Foundation. This support is gratefully acknowledged. The VSP data were collected as part of an environmental site study at Oakridge National Labs. The survey was conducted in cooperation with Bill Doll and Brad Carr of Oakridge National Labs and Bob Bainer of Lawrence Livermore National Labs.

References

Blonk, B., and Herman, G.C., 1994, Inverse scattering of surface waves: A new look at surface consistency: Geophysics, **59**, 963-972.

Bouchon, M., and Schmidt, D.P., 1989, Full-wave acoustic logging in an irregular borehole: Geophysics, **54**, 758-765.

Campbell, A.J., 1992, Tube wave attenuation by polarization filtering: 62nd Ann. Internat. Mtg., Soc. Expl. Geophys., Expanded Abstracts, 99-102.

Combee, L., 1994, Wavefield scattering by a 2-D near-surface elliptic anomaly: 64th Ann. Internat. Mtg., Soc. Expl. Geophys., Expanded Abstracts, 1306-1309.

Dong, Q., and Rector, J.W., 1997, Bi-domain modeling of borehole wave propagation: 67th Ann. Internat. Mtg., Soc. Expl. Geophys., Expanded Abstracts, 262-265.

Ellefsen, K.J., Burns, D.R., and Cheng, C.H., 1993, Homomorphic processing of the tube wave generated during acoustic logging: Geophysics, **58**, 1400-1407.

Hardage, B.A., 1981, Vertical seismic profiling, part A, principles: Geophysical Press.

Houston, L.M., 1992, Tube suppression: a comparison of median filtering and nearest-neighbor subtraction approaches: 62nd Ann. Internat. Mtg., Soc. Expl. Geophys., Expanded Abstracts, 128-132.

Mars, J.I., and Rector, J.W., 1995, Constrained eigenvectors: A means to separate aliased arrivals: 65th Ann. Internat. Mtg., Soc. Expl. Geophys., Expanded Abstracts, 49-52.

Milligan, P.A., Rector, J.W., and Bainer, R.W., 1997, Hydrophone VSP imaging at a shallow site: Geophysics, 62, 842-852.

Peng, C., and Toksöz, M.N., 1992, Tube wave generation at a layer boundary for an incident compressional plane wave: 62nd Ann. Internat. Mtg., Soc. Expl. Geophys., Expanded Abstracts, 213-216.

Pham, L.D., Krohn, C.E., Murray, T.J., and Chen, S.T., 1993, A tube wave suppression device for cross-well applications: 63rd Ann. Internat. Mtg., Soc. Expl. Geophys., Expanded Abstracts, 17-20.

Snieder, R., 1986a, 3D Linearized scattering of surface waves and a formalism for surface-wave holography: Geophys. J. R. astr. Soc., **84**, 581-601.

Snieder, R., 1986b, The influence of topography on the propagation and scattering of surface waves: Phys. Earth. Plan. Int., **44**, 226-241.

Stephen, R.A., Pardo-Casas, F., Cheng, C.H., 1985, Finite-difference synthetic acoustic logs: Geophysics, **50**, 1588-1609.

Tang, X.M., and Cheng, C.H., 1993, Borehole Stoneley wave propagation across permeable structures: Geophys. Prosp., **41**, 165-187.

Tezuka, K., Cheng, C.H., and Tang, X.M., 1997, Modeling of low-frequency Stoneley-wave propagation in an irregular borehole: Geophysics, **62**, 1047-1058.

Figure Captions

1. Arrival of the direct compressional wave for a simulated cross-well experiment in the region around a washout zone, located between depths of about 27 m and 30 m. The source is situated at the same depth as the washout zone. Due to the washout zone, a significant amount of scattered tube waves is generated that remains trapped in the washout zone for a while and therefore cause a severe distortion of the incoming wave.

2. Detail of the VSP. Between 90 m and 96 m depth, there is a significant amount of scattered tube waves present probably caused by a washout zone.

3. Same VSP as in figure 2, after applying a frequency-wavenumber fan filter removing all slopes equal or larger than the slope of the tube wave. The linear tube-wave noise has been removed, but the apex is still present between 90 m and 96 m.

4. Result after suppressing the downgoing direct arrival from the data shown in figure 3. In the washout zone, still remnants of the apex are visible in the form of events that are mainly present in this region and are smeared out by the repeated application of spatial filtering methods. They are interfering with the upcoming waves and therefore destroying the continuity of reflections in the washout zone.

5. "Undisturbed" direct arrival, d^0, that we would observe in the absence of the washout zone. This estimate has been obtained by applying a time window to the data of figure 2 and, subsequently, a narrow frequency-wavenumber fan filter in order to retain only the linear part of the direct arrival and therefore attributing rapid changes to tube-wave scattering.

6. Our estimate of the scattered first arrival, d^1, obtained after subtracting d^0 of figure 5 from the actual first arrival d.

7. Borehole scattering impedance $\sigma(z,t)$, obtained after applying a temporal inverse Fourier transfrom to $\sigma(z,\omega)$. The impedance has been obtained after applying a spatial deconvolution of the scattered direct arrival d^1 of figure 6 for the tube-wave Green's function. The impedance function is indeed more focussed than the scattered field d^1.

8. Estimate of the undisturbed wavefield p^0 we would observe in the absence of the washout zone. This result is obtained after predicting the scattered **total** field p^1 from the impedance function of figure 7, subtracting it from the total recorded field p and applying the same fan filter as in figure 3 for suppressing linear remnants of tube waves. The only difference with figure 3 is the removal of p^1; all other precessing and display parameters are the same in both figures. The impedance function has only been determined from the first arrival. Nevertheless, we observe that, also for the later arrivals not used in the derivation of the impedance filters, the interference patterns due to tube-wave scattering between 90 m and 96 m have been significantly attenuated in figure 8. This is an indication that the tube-wave scattering model is correct.

9. The result after removing the downgoing events from the result of 8. When we compare figure 9 with figure 4, we observe that the "wormy" interference patterns between 90 m and 96 m depth have been reduced whereas the continuity of upcoming events seems to have improved. The remaining interference patterns are probably due to the interference of events of different dip caused by the rather complex geology around the well.

10. Processed VSP after application of frequency-wavenumber filter for removing linear tube-wave noise and suppressing the direct arrival. The remnants of the tube-wave scattering apex are visible between 90 m and 96 m depth.

11. Same as figure 10 after, in addition, removal of the apex of the scattered tube-wave noise according to the method outlined in this paper. The reflections are more continuous between 90 m and 96 m depth.

Appendix: The one-dimensional Green's function

The one-dimensional Green's function used in Eq.(4) satisfies the one-dimensional Helmholtz equation with a point-source excitation, given by:

$$\left(\partial_z^2 \; + \; \frac{\omega^2}{c_T^2}\right) \; g(z-z',\omega) \; = \; -\delta(z-z') \; , \tag{8}$$

where c_T is the tube-wave velocity and δ is the Dirac delta function. It is given by

$$g(z-z',\omega) \; = \; \frac{\mathrm{e}^{-\mathrm{j}\omega|z-z'|/c_T}}{2\mathrm{j}\omega/c_T} \tag{9}$$

and consists of waves propagating away from the source at $z = z'$. In order to incorporate attenuation, we have taken the tube-wave velocity to be complex-valued, i.e.,

$$c_T \; = \; |c_T| \, (1 + \mathrm{j}\alpha) \quad (\alpha \geq 0) \; , \tag{10}$$

with $\alpha \approx 0.1$. In the computations shown in section 3, the factor $2\mathrm{j}\omega/c_T$ has been disgarded and is therefore incorporated in the image of the borehole impedance function σ.

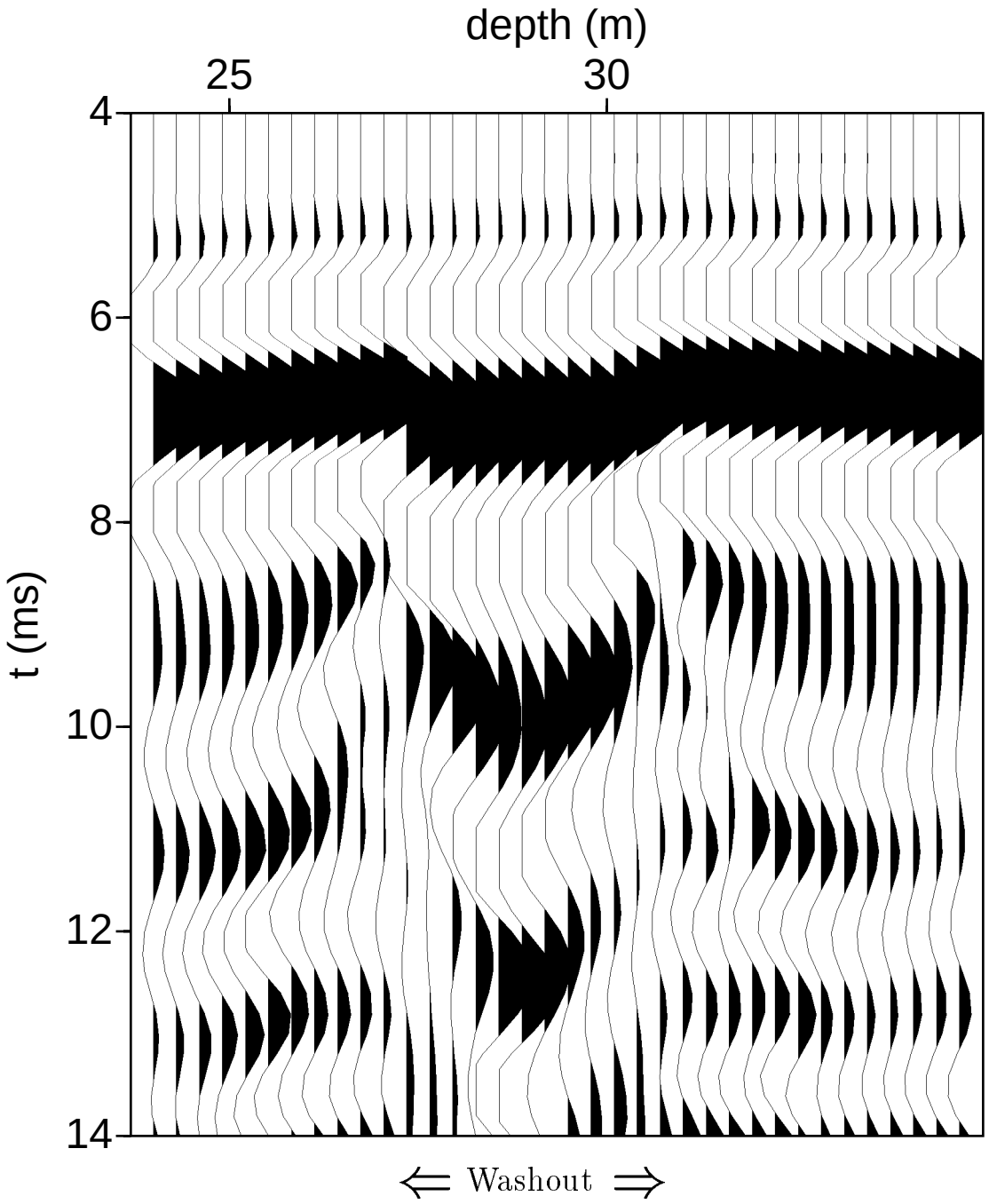

Figure 1: Arrival of the direct compressional wave for a simulated cross-well experiment in the region around a washout zone, located between depths of about 27 m and 30 m. The source is situated at the same depth as the washout zone. Due to the washout zone, a significant amount of scattered tube waves is generated that remains trapped in the washout zone for a while and therefore cause a severe distortion of the incoming wave.

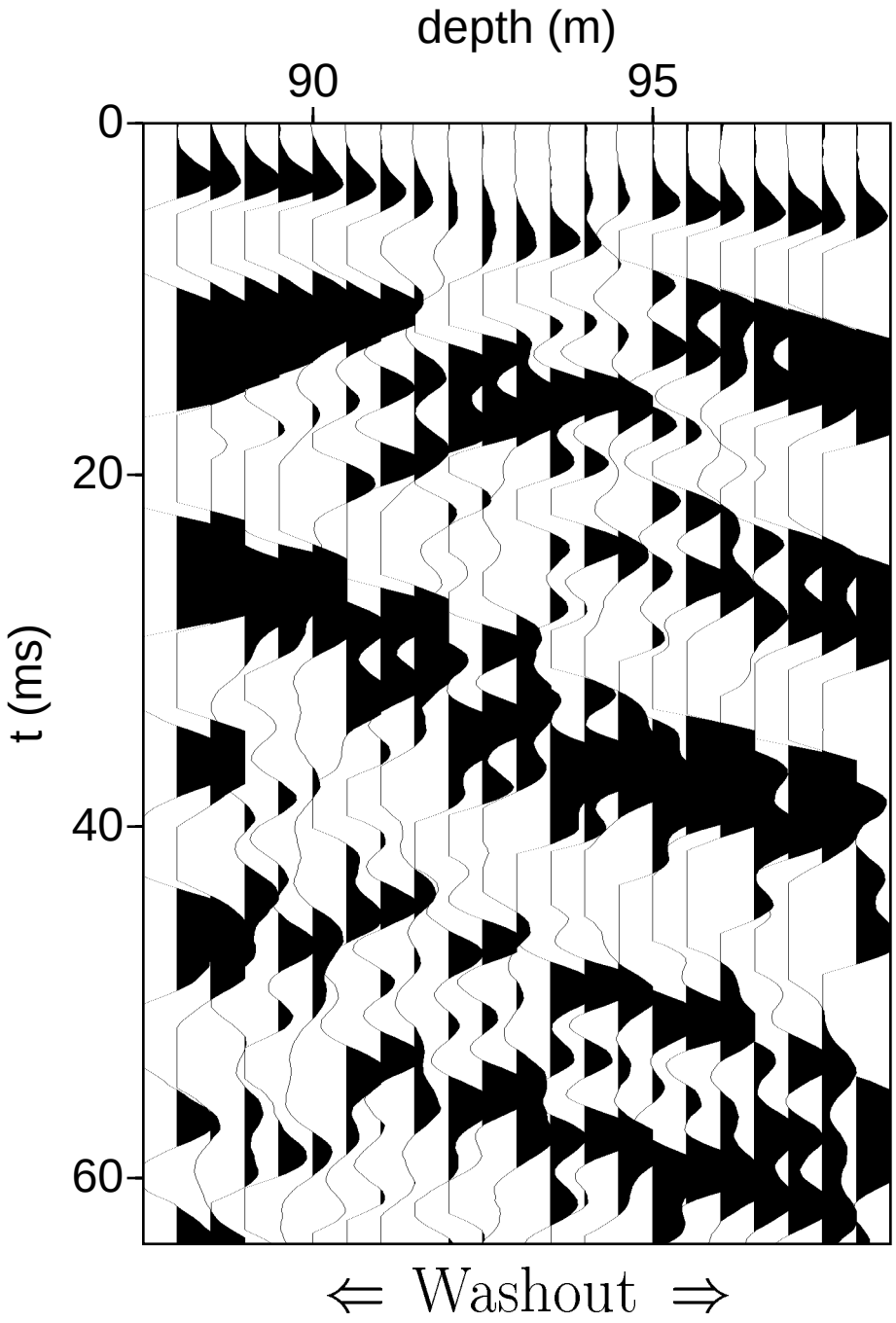

Figure 2: Detail of the VSP. Between 90 m and 96 m depth, there is a significant amount of scattered tube waves present probably caused by a washout zone.

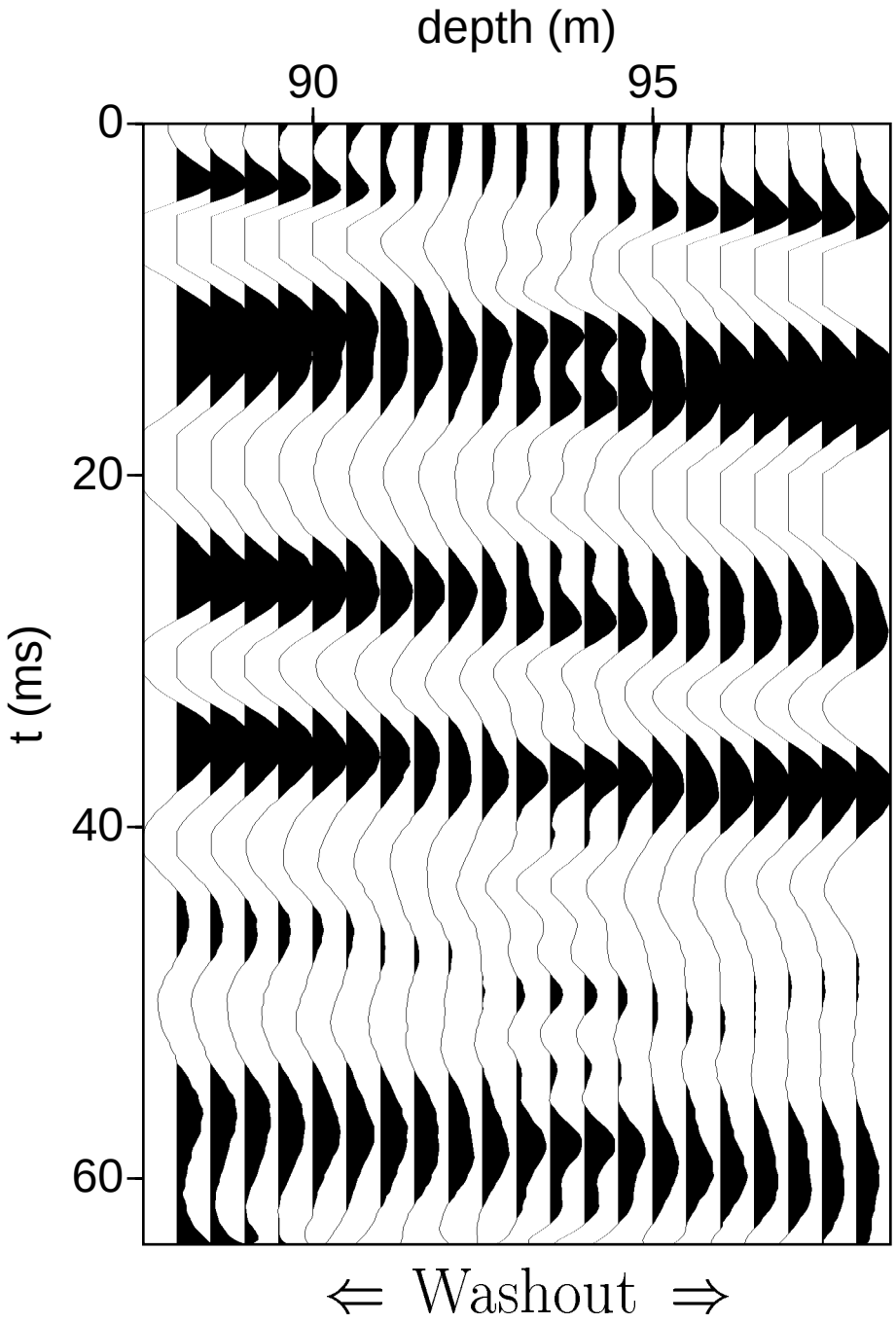

Figure 3: Same VSP as in figure 2, after applying a frequency-wavenumber fan filter removing all slopes equal or larger than the slope of the tube wave. The linear tube-wave noise has been removed, but the apex is still present between 90 m and 96 m.

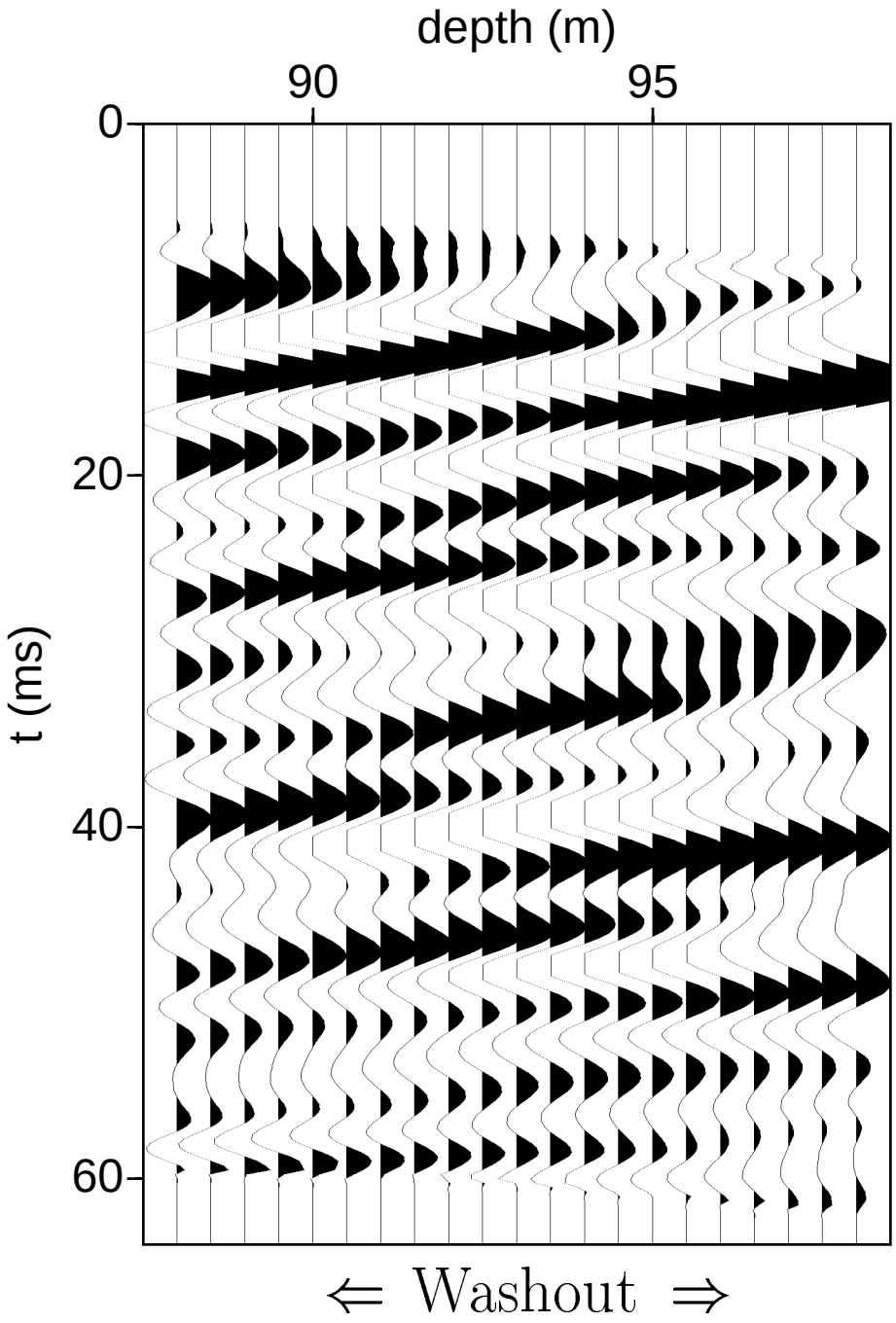

Figure 4: Result after suppressing the downgoing direct arrival from the data shown in figure 3. In the washout zone, still remnants of the apex are visible in the form of events that are mainly present in this region and are smeared out by the repeated application of spatial filtering methods. They are interfering with the upcoming waves and therefore destroying the continuity of reflections in the washout zone.

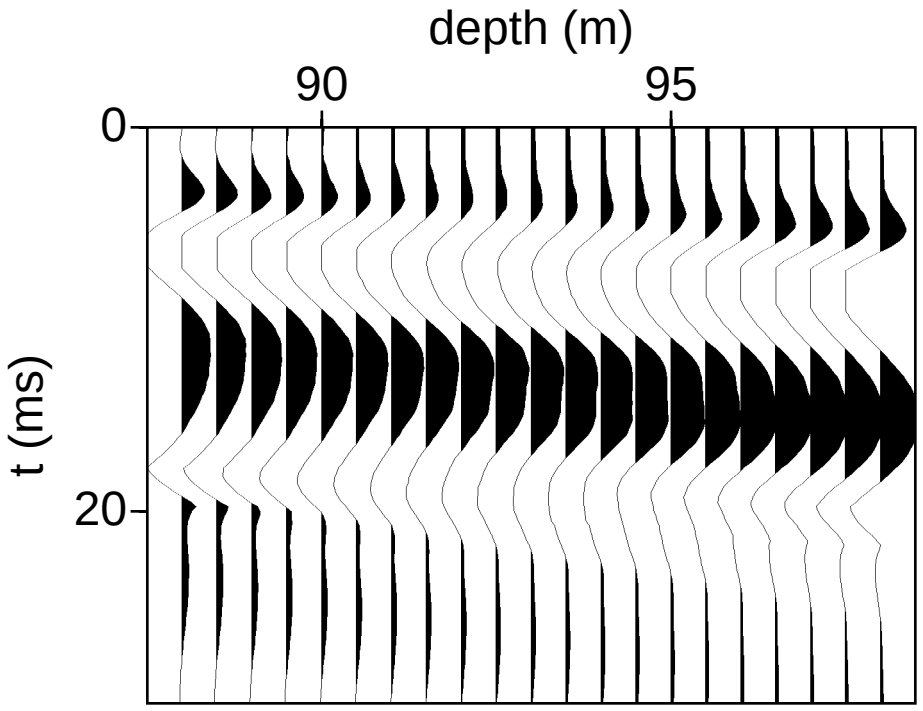

Figure 5: "Undisturbed" direct arrival, d^0, that we would observe in the absence of the washout zone. This estimate has been obtained by applying a time window to the data of figure 2 and, subsequently, a narrow frequency-wavenumber fan filter in order to retain only the linear part of the direct arrival and therefore attributing rapid changes to tube-wave scattering.

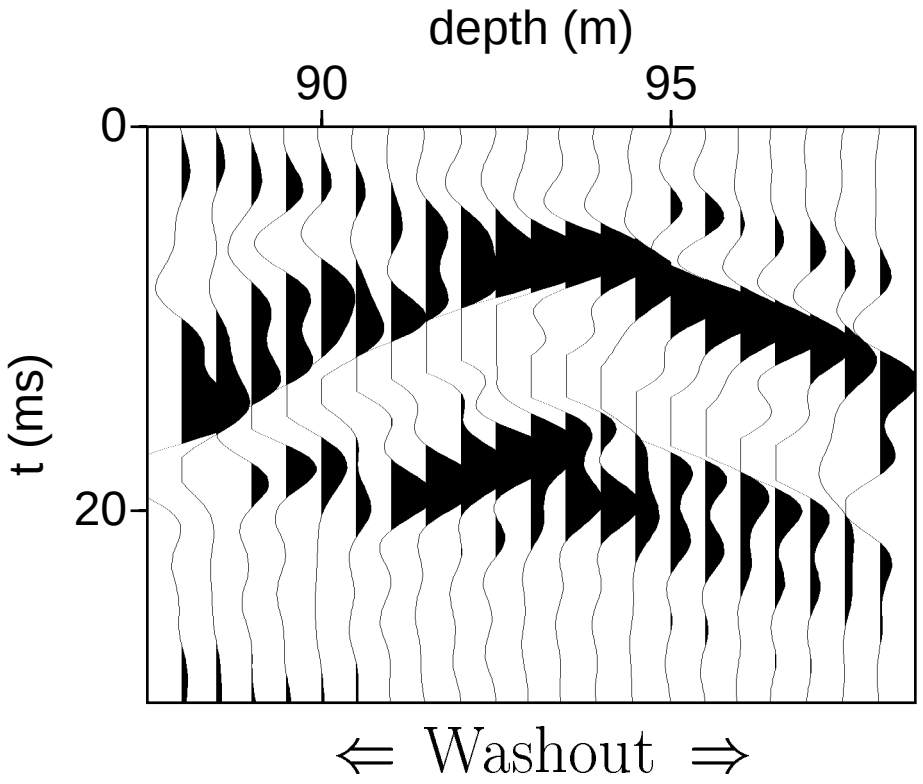

Figure 6: Our estimate of the scattered first arrival, d^1, obtained after subtracting d^0 of figure 5 from the actual first arrival d.

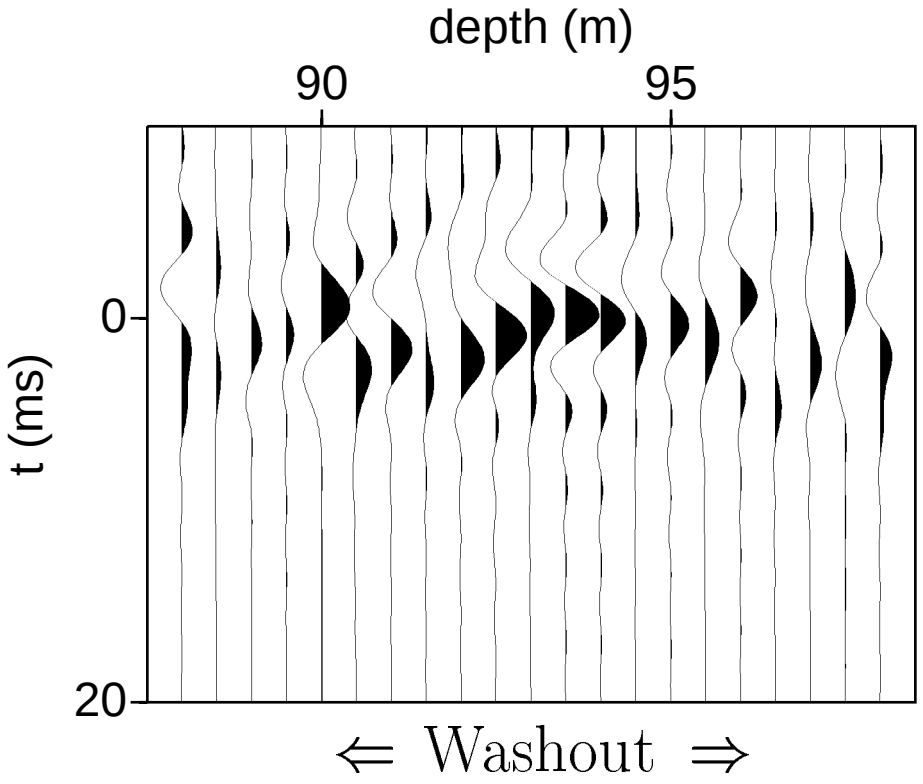

Figure 7: Borehole scattering impedance $\sigma(z,t)$, obtained after applying a temporal inverse Fourier transfrom to $\sigma(z,\omega)$. The impedance has been obtained after applying a spatial deconvolution of the scattered direct arrival d^1 of figure 6 for the tube-wave Green's function. The impedance function is indeed more focussed than the scattered field d^1.

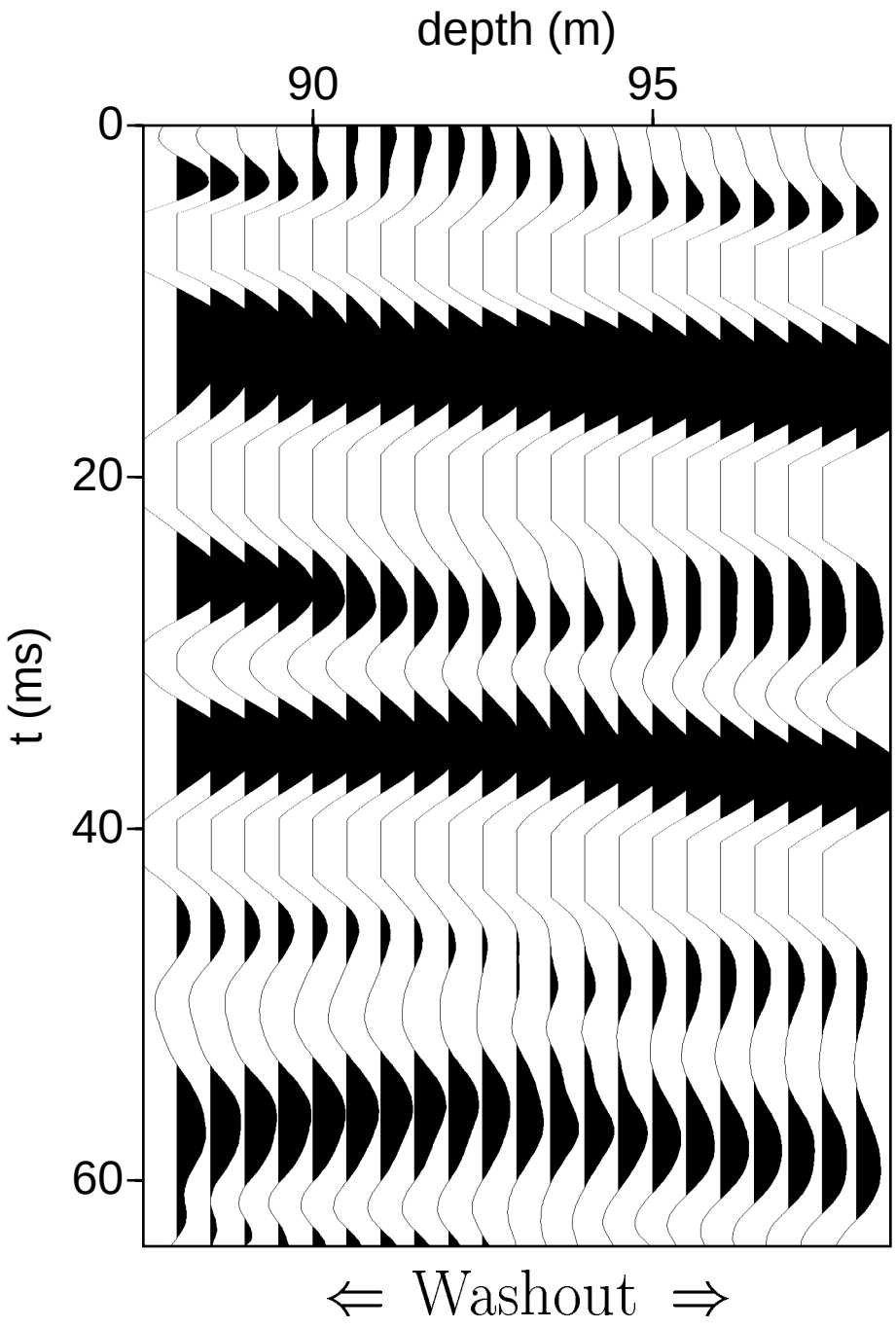

Figure 8: Estimate of the undisturbed wavefield p^0 we would observe in the absence of the washout zone. This result is obtained after predicting the scattered **total** field p^1 from the impedance function of figure 7, subtracting it from the total recorded field p and applying the same fan filter as in figure 3 for suppressing linear remnants of tube waves. The only difference with figure 3 is the removal of p^1; all other precessing and display parameters are the same in both figures. The impedance function has only been determined from the first arrival. Nevertheless, we observe that, also for the later arrivals not used in the derivation of the impedance filters, the interference patterns due to tube-wave scattering between 90 m and 96 m have been significantly attenuated in figure 8. This is an indication that the tube-wave scattering model is correct.

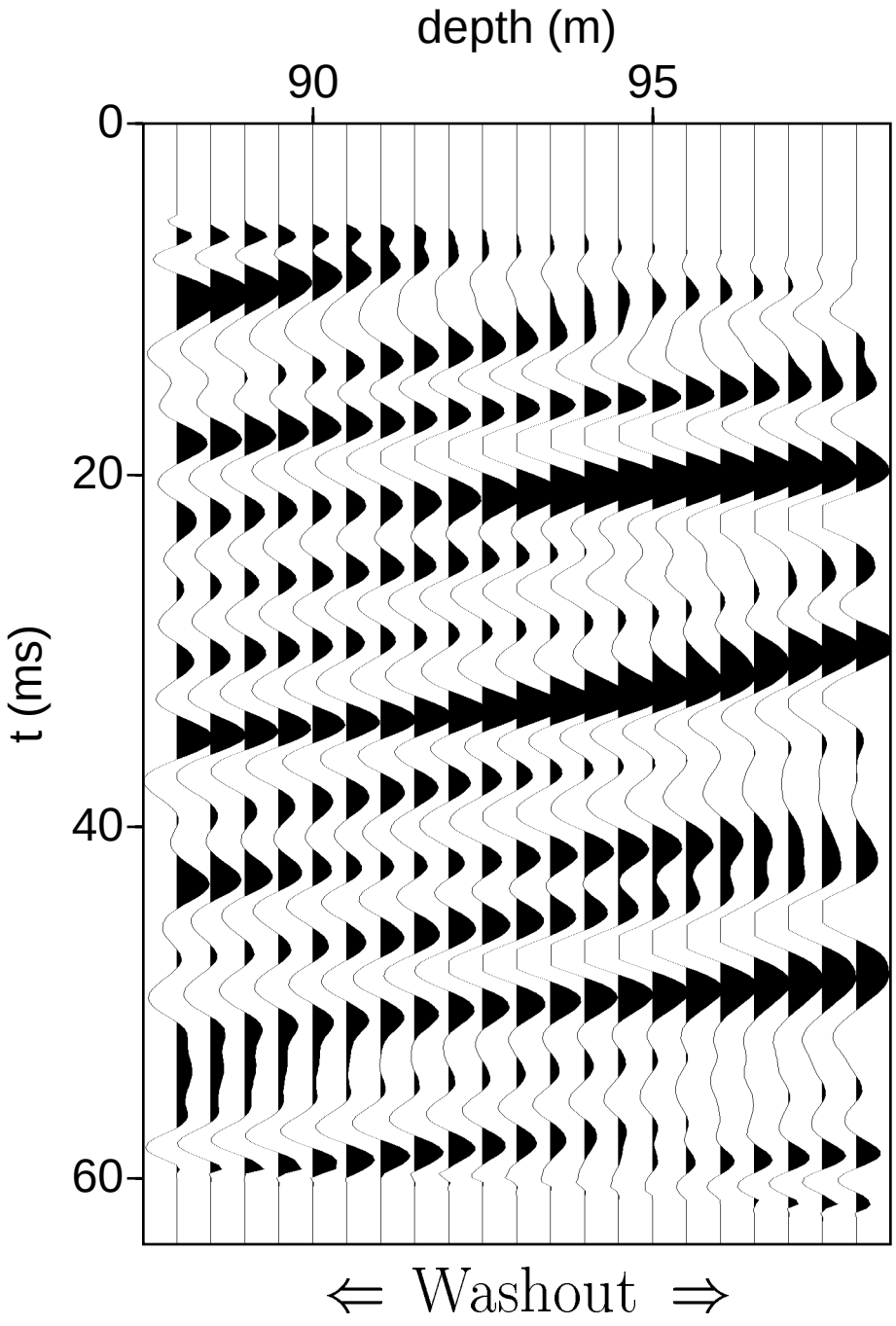

Figure 9: The result after removing the downgoing events from the result of 8. When we compare this figure with figure 4, we observe that the "wormy" interference patterns between 90 m and 96 m depth have been reduced whereas the continuity of upcoming events seems to have improved. The remaining interference patterns are probably due to the interference of events of different dip caused by the rather complex geology around the well.

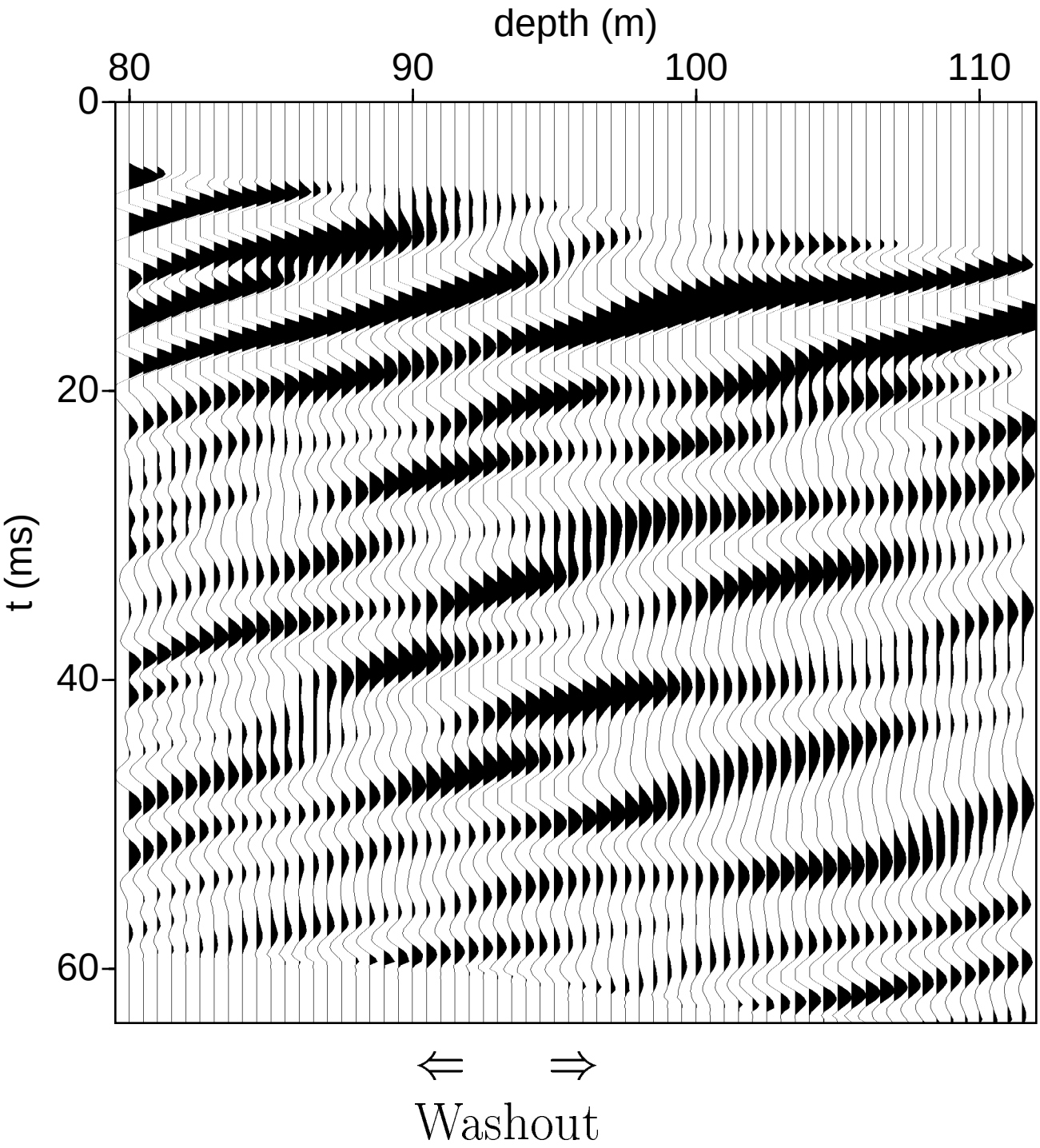

Figure 10: Processed VSP after frequency-wavenumber filter for removing linear tube-wave noise and suppressing the direct arrival. The remnants of the tube-wave scattering apex are visible between 90 m and 96 m depth.

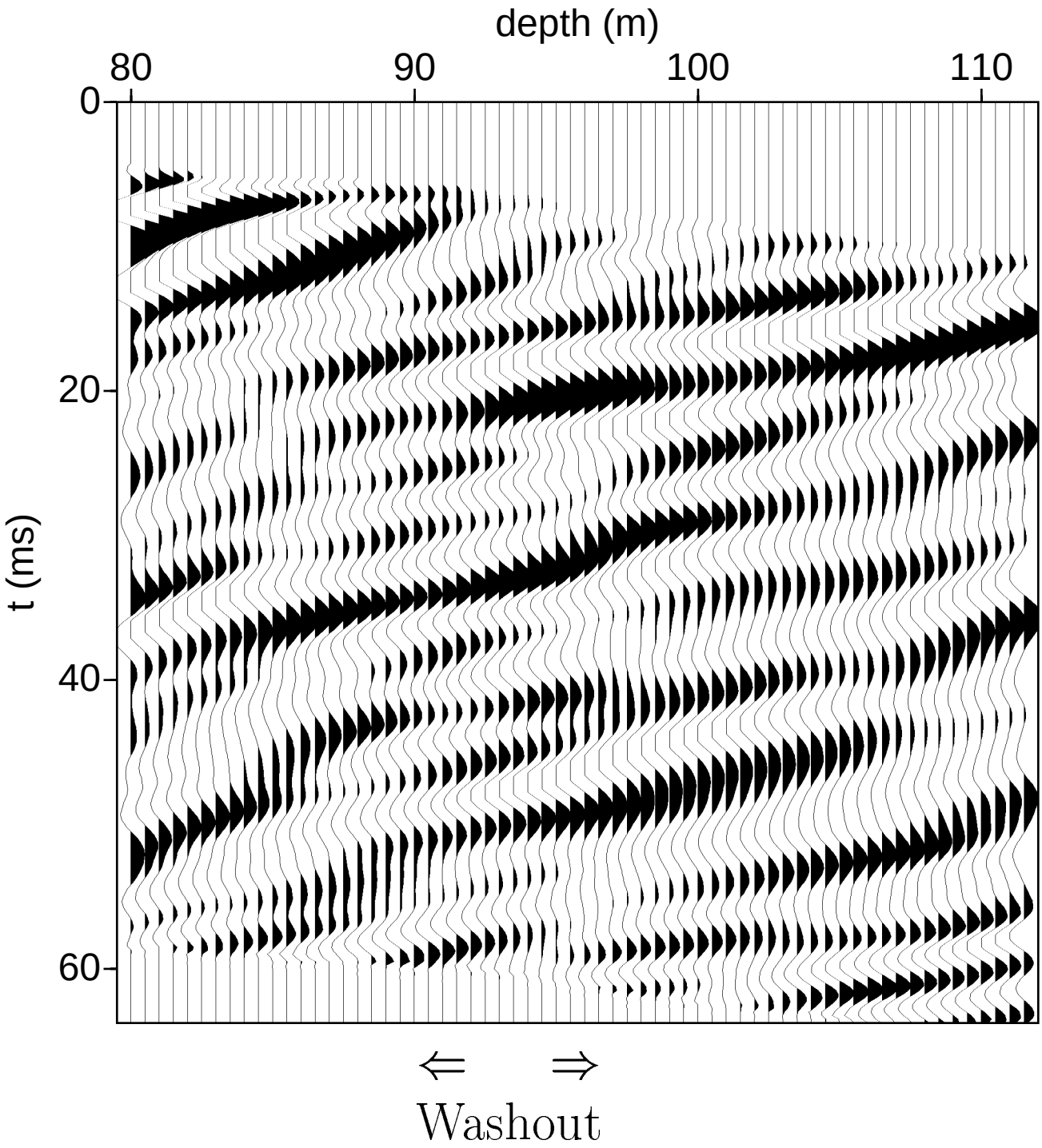

Figure 11: Same as figure 10 after, in addition, removal of the apex of the scattered tube-wave noise according to the method outlined in this paper. The reflections are more continuous between 90 m and 96 m depth.